

Chapter 4: Immersed Body Flow

[pp. 445-459 (8e), or 374-386 (9e)]

Dr. Bing-Chen Wang

Dept. of Mechanical Engineering

Univ. of Manitoba, Winnipeg, MB, R3T 5V6

When a viscous fluid flow passes a solid body (fully-immersed in the fluid), the body experiences a net force, \mathbf{F} , which can be decomposed into two components:

- a **drag force** F_D , which is parallel to the flow direction, and
- a **lift force** F_L , which is perpendicular to the flow direction.

The **drag coefficient** C_D and **lift coefficient** C_L are defined as follows:

$$\boxed{C_D = \frac{F_D}{\frac{1}{2}\rho U^2 A}} \quad \text{and} \quad \boxed{C_L = \frac{F_L}{\frac{1}{2}\rho U^2 A_p}} \quad , \quad (112)$$

respectively. Here, U is the free-stream velocity, A is the “**wetted area**” (total surface area in contact with fluid), and A_p is the “**planform area**” (maximum projected area of an object such as a wing).

In the remainder of this section, we focus our attention on the drag forces. As discussed previously, there are two types of drag forces acting on a solid body immersed in a viscous flow:

- **friction drag** (also called “**viscous drag**”), due to the wall friction shear stress exerted on the surface of a solid body;
- **pressure drag** (also called “**form drag**”), due to the difference in the pressure exerted on the front and rear surfaces of a solid body.

The friction drag and pressure drag on a finite immersed body are defined as

$$\boxed{F_{D,vis} = \int_A \tau_w dA} \quad \text{and} \quad \boxed{F_{D,pres} = \left(\int_A p dA \right)_{\text{Streamwise component}}} \quad , \quad (113)$$

respectively. In an inviscid flow, the total drag force exerted on a solid body is solely contributed by the pressure drag. However in a viscous flow, the total drag force is often a combination of both friction and pressure drags, i.e.

$$\boxed{F_D = F_{D,vis} + F_{D,pres}} \quad , \quad (114)$$

and in consequence,

$$\boxed{C_D = C_{D,vis} + C_{D,pres}} \quad . \quad (115)$$

2.6. Friction Drag for Flow over a Flat Plate with Zero Incidence

In this subsection, we consider the drag forces for a flow past a finite flat plate with zero incidence (i.e., the flow is parallel to the flat plate). The drag coefficient C_D will be investigated according to the following three scenarios of BLs developed over the flat plate: (1) a laminar BL, (2) a turbulent BL, and (3) a laminar-to-turbulent transition BL.

For a BL flow past over a finite flat plate (see Fig. 16), the drag coefficient C_D relates to the local skin friction coefficient C_f as

$$C_D = \frac{F_D}{\frac{1}{2}\rho U^2 A} = \frac{\int_A \tau_w dA}{\frac{1}{2}\rho U^2 A} = \boxed{\frac{1}{A} \int_A C_f dA} \quad . \quad (116)$$

To derive the above equation, we used the definition of the local skin friction coefficient: $C_f = \frac{\tau_w}{\frac{1}{2}\rho U^2}$.

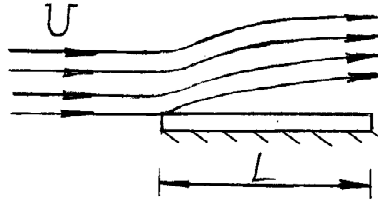


Fig. 16: A finite flat plate parallel to a viscous flow. The length and depth of the plate are L and b , respectively. The drag force is contributed by the wall friction drag only.

(1) Laminar BL over a Finite Flat Plate

As demonstrated previously in Table 9.2 (see page 47), the exact solution on the local skin coefficient C_f for a laminar BL is

$$C_f = \frac{\tau_w}{\frac{1}{2}\rho U^2} = \frac{0.664}{\sqrt{Re_x}} \quad . \quad (117)$$

Substituting this equation into Eq. (116), we have

$$C_D = \frac{1}{A} \int_A \frac{0.664}{\sqrt{Re_x}} dA = \frac{1}{bL} \int_0^L 0.664 \left(\frac{U}{\nu}\right)^{-0.5} x^{-0.5} \cdot b dx = 1.33 \left(\frac{\nu}{UL}\right)^{0.5} \quad , \quad (118)$$

or,

$$\boxed{C_D = \frac{1.33}{\sqrt{Re_L}}} \quad (\text{for a laminar BL}) \quad , \quad (\text{Eq. (9.33) in textbook})$$

where $\boxed{Re_L = \frac{UL}{\nu}}$, and L and b represent the length and the depth of the flat plate, respectively.

(2) Turbulent BL over a Finite Flat Plate

As derived previously (on page 51), the local skin friction coefficient for a turbulent BL over a flat plate is given by Eq. (93), i.e.

$$C_f = \frac{\tau_w}{\frac{1}{2}\rho U^2} = \frac{0.0594}{Re_x^{1/5}} \quad . \quad (93)$$

Substituting the equation into Eq. (116), we have

$$C_D = \frac{1}{A} \int_A \frac{0.0594}{Re_x^{1/5}} dA = \frac{1}{bL} \int_0^L 0.0594 \left(\frac{U}{\nu}\right)^{-0.2} x^{-0.2} \cdot b dx = 0.0742 \left(\frac{\nu}{UL}\right)^{0.2} \quad , \quad (119)$$

or,

$$\boxed{C_D = \frac{0.0742}{Re_L^{1/5}}} \quad (\text{for a turbulent BL, valid for } 5 \times 10^5 < Re_L < 10^7) \quad , \quad (\text{Eq. (9.34) in textbook})$$

For $Re_L < 10^9$, Schlichting gives the following semi-empirical equation for a turbulent viscous flow over a finite flat plate

$$C_D = \frac{0.455}{(\log Re_L)^{2.58}} \quad , \quad (\text{Eq. (9.35) in textbook})$$

which fits experimental data very well.

(3) Laminar-to-Turbulent Transition BL over a Finite Flat Plate

For a BL experiencing transition from laminar to turbulent pattern, the value of C_D based on the

turbulent BL (cf. Eq. (9.34) and Eq. (9.35) in textbook) needs to be corrected to account for the initial laminar BL effect. If the transition Reynolds number is 5×10^5 , the drag coefficient is

$$C_D = \frac{0.0742}{Re_L^{1/5}} - \underbrace{\frac{1740}{Re_L}}_{\text{correction}} \quad (\text{for } 5 \times 10^5 < Re_L < 10^7) \quad , \quad (\text{Eq. (9.37a) in textbook})$$

or,

$$C_D = \frac{0.455}{(\log Re_L)^{2.58}} - \underbrace{\frac{1610}{Re_L}}_{\text{correction}} \quad (\text{for } 5 \times 10^5 < Re_L < 10^9) \quad . \quad (\text{Eq. (9.37b) in textbook})$$

Figure 17 plots the drag coefficient for a BL which transitions from laminar to turbulent pattern at $Re_x = 5 \times 10^5$ for a viscous flow past a flat plate. The values of drag coefficient C_D for the laminar BL (cf. Eq. (9.33) in textbook), turbulent BL (cf. Eqs. (9.34) and (9.35) in textbook) and transition BL (cf. Eqs. (9.37b) in textbook), are demonstrated and compared in the figure. From Fig. 17, it is clear that for a viscous BL flow over a finite flat plate:

- viscous drag is significant when Re_L is low;
- at a given Re_L (for a given length of the plate L and a given free-stream velocity U), the value of C_D is less for a laminar BL; implying that for a given length of the plate, the drag coefficient is less, when laminar flow is maintained over the longest possible distance;
- at large $Re_L (> 10^7)$, the effects of the initial laminar BL on C_D can be ignored.

2.7. Pressure Drag

Figure 18 shows a viscous flow past a finite flat plate (perpendicular to the flow). The friction drag over the plate is zero, because the plate is perpendicular to the flow. The drag force is contributed by the pressure drag only, which is

$$F_D = \left(\int_A p dA \right)_{\text{Streamwise component}} \quad . \quad (120)$$

When flow passes an object with sharp edges, BL separation is triggered and wake is induced. The drag coefficient for all objects with sharp edges is essentially independent of Reynolds number

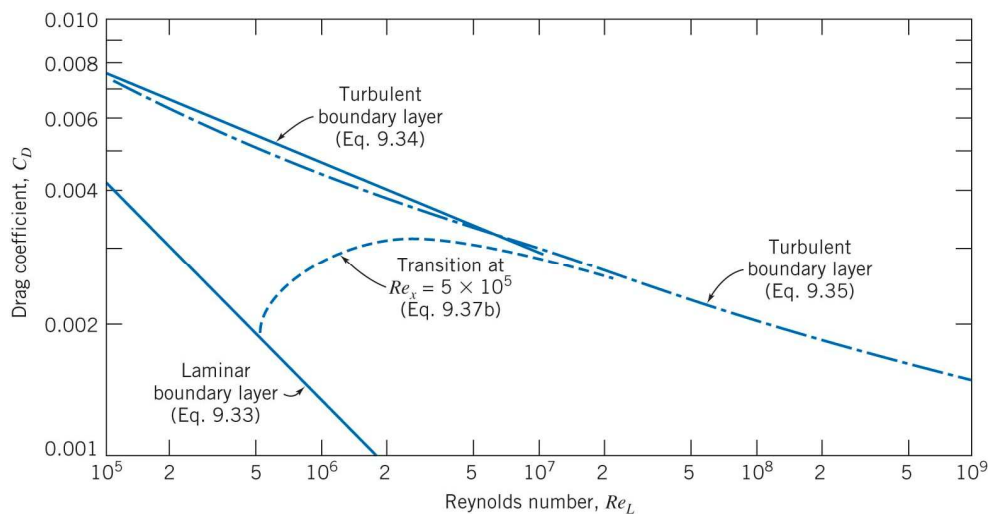


Fig. 17: Variation of drag coefficient C_D with Reynolds number Re_L for a smooth flat plate parallel to a viscous flow.

(for $Re > 1000$) because the size of the wake is fixed by the geometry of the object. Drag coefficients for some selected sharp-edged objects (for $Re > 1000$) are given in Table 9.3.

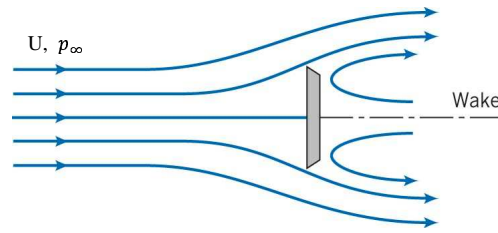


Fig. 18: A finite flat plate perpendicular to a viscous flow. The friction drag is zero (because the plate is perpendicular to the flow), and the drag force is contributed by the pressure drag only.

Table 9.3

Drag Coefficient Data for Selected Objects ($Re \geq 10^3$)^a

Object	Diagram	$C_D(Re \geq 10^3)$
Square prism		$b/h = \infty$ 2.05
		$b/h = 1$ 1.05
Disk		1.17
Ring		1.20 ^b
Hemisphere (open end facing flow)		1.42
Hemisphere (open end facing downstream)		0.38
C-section (open side facing flow)		2.30
C-section (open side facing downstream)		1.20

^aData from Hoerner [16].

^bBased on ring area.

2.8. Combined Friction & Pressure Drag: for Flow over a Sphere or Cylinder

In the case of a flow over a sphere or a cylinder, both friction drag and pressure drag contribute to the total drag, i.e. $F_D = F_{D,pres} + F_{D,vis}$. However, the contributions from $F_{D,pres}$ and $F_{D,vis}$ to the total drag F_D depend upon the Reynolds number and surface roughness (such as dimples on a golf ball).

► at a very low Reynolds number for $Re \leq 1$, Stokes showed analytically that there is no flow separation from a sphere, the wake is laminar and the drag is predominantly the friction drag, and the total drag coefficient is

$$C_D = \frac{24}{Re} \quad , \quad (121)$$

which is plotted in Fig. 19. From the figure, it is clear that the above analytical result of Stokes deviates from experimental data if $Re > 1$.

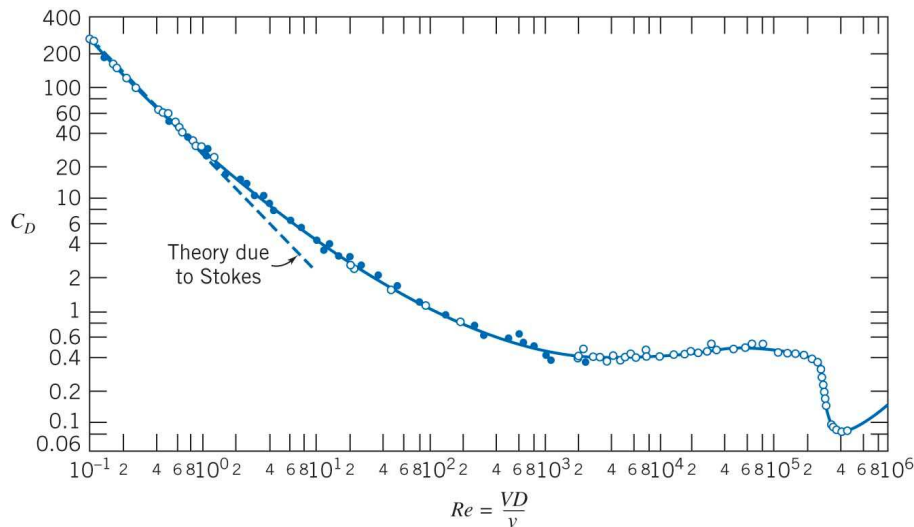


Fig. 19: (Fig. 9.11 in the textbook) Drag coefficient C_D of a smooth sphere as a function of Reynolds number Re .

► Fig. 19 shows that as Re increases, C_D decreases. At $Re \approx 1000$, 95% of the total drag is due to the pressure drag. For $1000 < Re < 3 \times 10^5$, C_D is approximately constant (i.e., C_D is approximately independent of Re). If $C_D \approx \text{constant}$, $F_D = C_D \cdot (\frac{1}{2}\rho U^2)A \Rightarrow F_D \propto U^2$, indicating a rapid increase in drag in response to the magnitude of U .

► If $Re > 3 \times 10^5$, transition occurs and the BL on the forward portion of the sphere becomes turbulent. The point of separation then moves downstream and the size of the wake decreases. Therefore, the net pressure drag is reduced.

The effects of a laminar BL and a turbulent BL over a smooth ball are compared in Fig. 20. Furthermore, the result of the inviscid flow is also shown.

- For an inviscid flow, pressure drag is the only drag (viscous drag is zero identically because $\mu \equiv 0$). Because the pressure is symmetrically distributed (w.r.t. θ) around the sphere, the total drag (purely due to the pressure drag) in an inviscid flow is zero identically, leading to the so-called “d’Alembert’s paradox” (which states that for an inviscid flow, the drag of any body of any shape immersed in a uniform stream is identically zero).

- For the viscous laminar BL flow, the BL separation occurs around $\theta = 82^\circ$; and for the turbulent BL flow, the BL separation is delayed to approximately $\theta = 120^\circ$. In the turbulent case, the low pressure wake region is much reduced. Therefore, the pressure drag due to the pressure difference between the front and rear of a sphere is greatly reduced.

Figure 21 compares flow separation patterns of a laminar BL over a smooth ball and a turbulent BL over a rough ball. The dimples on the rough ball triggers the onset of turbulence. The turbulent BL delays the BL separation, and therefore, makes the low pressure wake region much narrower, resulting in a much reduced pressure drag. With a reduced drag force, a golf ball can fly over a much longer distance than a smooth ball! The key is to use dimples to trigger the onset of a turbulent BL.

Figure 22 shows the drag coefficient for flow over a smooth cylinder. The distribution of C_D around the circular cylinder is similar to that around a sphere shown previously in Fig. 19. However, the value of C_D for a smooth cylinder is about twice higher than that for a smooth sphere.

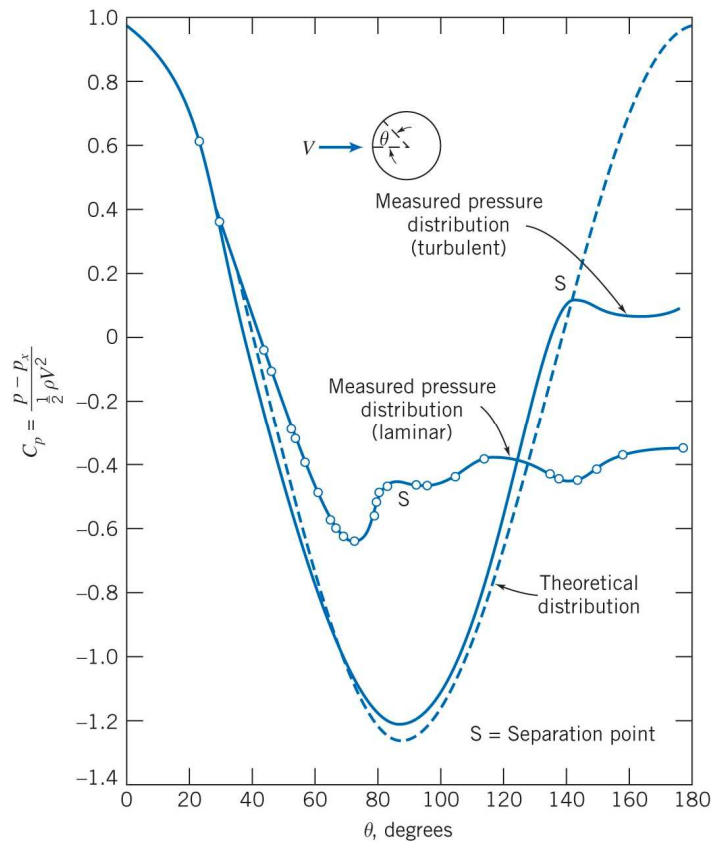


Fig. 20: Pressure distribution around a smooth sphere for laminar and turbulent BL flow, compared with the inviscid flow result. For the inviscid flow, the pressure coefficient $C_p = \frac{p - p_\infty}{\frac{1}{2}\rho U^2} = 1 - 4 \sin^2 \theta$, which represents a symmetrical distribution around the sphere. For the viscous laminar BL flow, the BL separation occurs around $\theta = 82^\circ$; and for the turbulent BL flow, the BL separation is delayed to approximately $\theta = 120^\circ$.

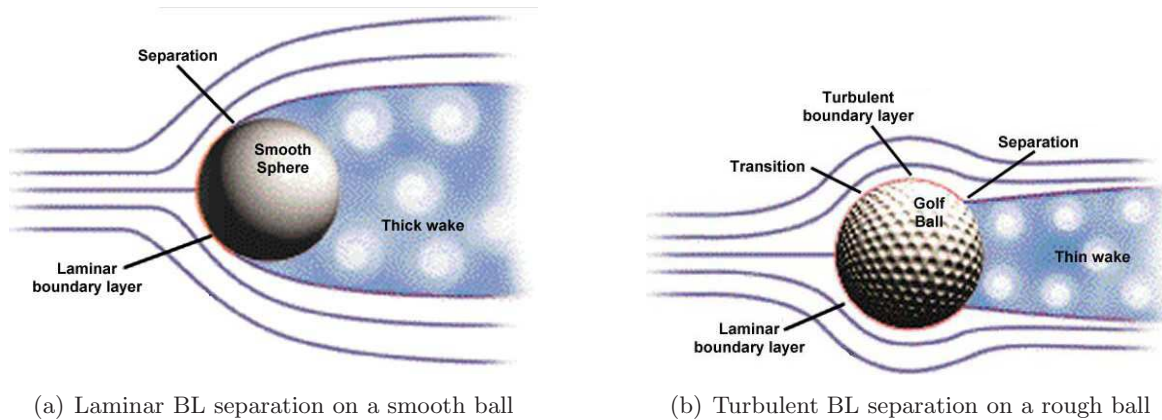


Fig. 21: Flow separation on a sphere with laminar and turbulent BLs (source of figure [8]). The dimples on the rough (golf) ball triggers the onset of turbulence. The turbulent BL delays the BL separation, and therefore, makes the low pressure wake region much narrower. As a result, the pressure drag due to the pressure difference between the front and back of the sphere is greatly reduced.

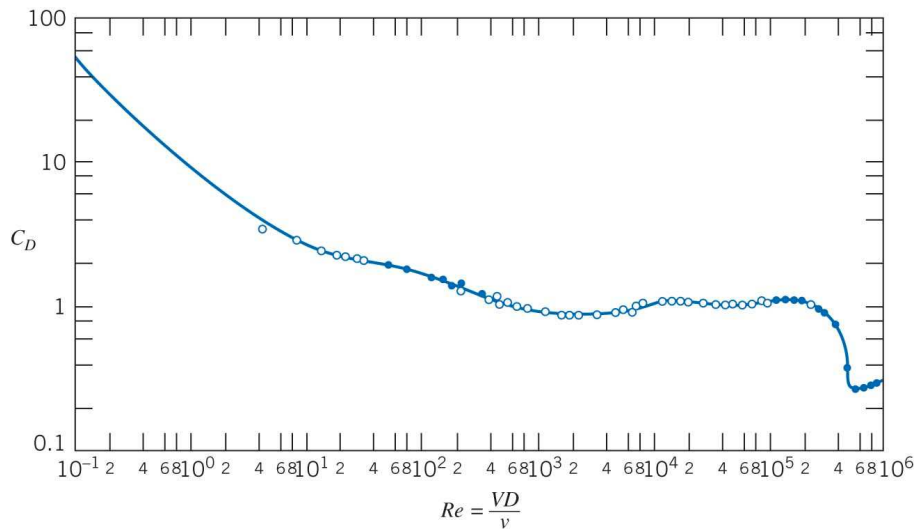


Fig. 22: (Fig. 9.13 in the textbook) Drag coefficient C_D of a smooth circular cylinder as a function of Reynolds number Re .

Characteristic Area in Drag Coefficient

The drag coefficient is defined based on a **characteristic area** A , i.e.

$$C_D = \frac{F_D}{\frac{1}{2}\rho V^2 A} \quad .$$

When we use this equation, the characteristic area A assumes one of the following three types:

- ▶ **Wetted area** (i.e. the total surface area that is in contact with fluid), typically for calculation of the wall friction drag over the surface of a flat plate or a ship.
- ▶ **Frontal area** (i.e. the projected area as seen by the flow), typically for calculation of aerodynamic drag over a thick blunt bluff body such as a cylinder, a car, and a hemisphere. Calculations involving Table 9.3, Fig. 9.11 and Fig. 9.13 (of the textbook) are usually based on the frontal area.
- ▶ **Planform area** (i.e. the maximum projected area as seen from above), typically for calculation of aerodynamic drag and lift for a wide flat body such as a wing or a hydrofoil.

2.9. Streamlining

The extent of the wake (separated flow region) behind an object can be reduced or even eliminated by using streamlining (based on proper body shapes), which in turn significantly reduces the pressure drag. The speed of flows around a moving object (e.g., flow past an airplane or a truck) is typically very high (in consequence, the value of Re is very high) in many engineering cases, and therefore, the most dominant form of drag is typically caused by the pressure drag. The streamlining technique can be the key to reduce the pressure drag.

Figure 23 compares the flow separation patterns of a blunt body and a streamlined “teardrop” shaped-body. The streamlined teardrop shape creates a much more gradual adverse pressure gradient. The much less severe pressure gradient then promotes attached flow much further along the body to reduce/eliminate flow separation. Figure 24 shows truck model 587 manufactured by the Peterbilt Motors Company. This truck has been thoroughly tested in terms of aerodynamic performances. The streamlined hood and molded bumper smoothly divert airflow around the vehicle and trailer in order

to minimize flow separation and pressure drag.

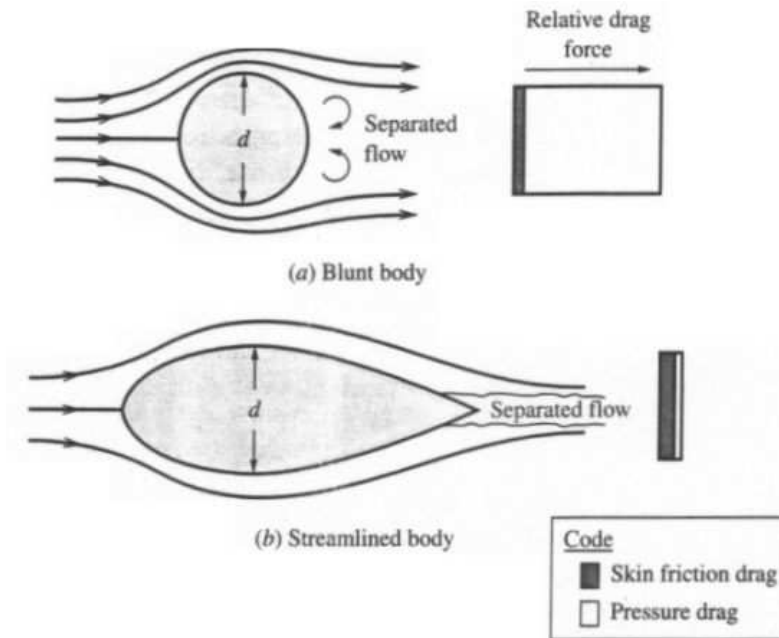


Fig. 23: Comparison of flow separation and drag on blunt and streamlined shapes (source of figure [2]).

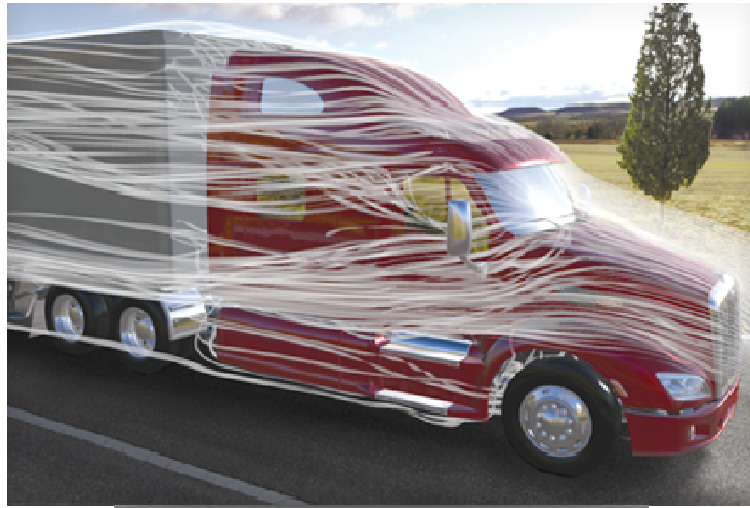


Fig. 24: Truck model 587 manufactured by Peterbilt Motors Company (based in Denton, Texas). According to the company sales advertisement, “this truck model is innovatively designed for those who demand outstanding aerodynamic performance, superior fuel efficiency and the highest overall value. A streamlined hood and molded bumper smoothly divert airflow around the vehicle and trailer. Extensive wind tunnel testing and computational fluid dynamics have proven a 1.25% fuel-efficiency gain. The model 587 is SmartWay designated by the EPA as fuel efficient and environmentally friendly” (source of figure [3]).

Interesting web links related to aerodynamic drag:

Aeroflexible aerodynamics: <https://www.youtube.com/watch?v=Nbk8zSRCytA>

Bus flow and design: https://www.youtube.com/watch?v=_NPNIyR5cWo

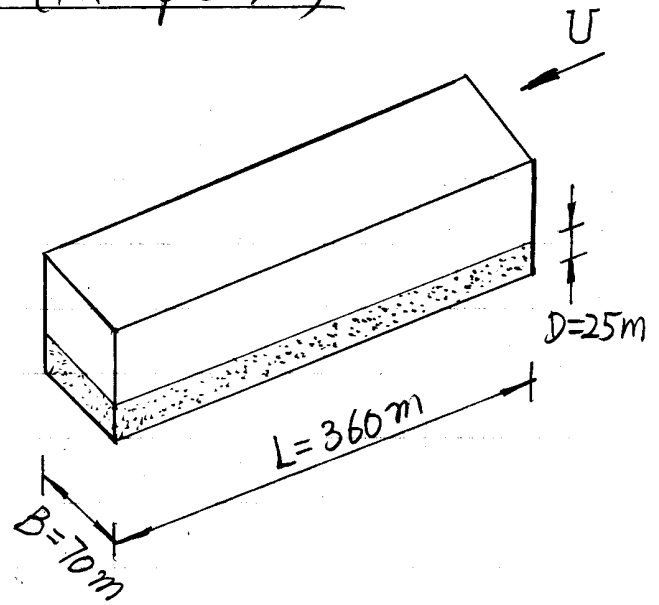
Speedo research (skin friction): <https://www.youtube.com/watch?v=dvMdqvO3R9g>

REFERENCES

- [1] Pritchard, P. J. 2011, *Fox and McDonald's Introduction to Fluids Mechanics*, 8th edition, Wiley, USA.
- [2] Aerospaceweb.org, 2007-2012, <http://www.aerospaceweb.org/>.
- [3] Peterbilt Motors Company 2013, <http://www.peterbilt.com/>.

Example on Skin Friction Drag (Example 9.5)

Given: Supertanker with
 $L=360\text{ m}$, $B=70\text{ m}$,
 Draft $D=25\text{ m}$
 $U=13\text{ kt}$
 $T=10^\circ\text{C}$ seawater



Find: (a) Force required to overcome skin friction Drag
 (b) Power

Solution:

(a) Reynolds number

$$U = 13\text{ kt}$$

$$= 13 \times 6076.17 \times 0.3048 \times \frac{1}{3600}$$

$$= 6.688\text{ (m/s)}$$

1 kt = 1 Nautical Mile Per hour
 or, 1 kt = 1 nm/hr
 1 nm = 6076.17 ft
 1 ft = 0.3048 m (or, 30.48 cm)

From Appendix A, at 10°C , $\nu = 1.37 \times 10^{-6}\text{ m}^2/\text{s}$ for seawater

$$Re_L = \frac{UL}{\nu} = \frac{6.688 \times 360}{1.37 \times 10^{-6}} = 1.757 \times 10^9$$

Considering the value of Re_L , we need to use Eq. (9.376) to estimate the drag coefficient

$$C_D = \frac{0.455}{(\log Re_L)^{2.58}} - \frac{1610}{Re_L}$$

$$= \frac{0.455}{(\log 1.757 \times 10^9)^{2.58}} - \frac{1610}{1.757 \times 10^9}$$

$$= 0.00147$$

Also, consider that

$$C_D = \frac{F_D}{\frac{1}{2} \rho U^2 A}$$

$$\therefore F_D = C_D \cdot \frac{1}{2} \rho U^2 A$$

the wetted width = $B + 2D$

the wetted area: $A = L \cdot (B + 2D) = 360 \times (70 + 25 \times 2) = 43200 \text{ (m}^2\text{)}$

Density of seawater $\rho = 1020 \text{ kg/m}^3$

$$\therefore F_D = C_D \cdot \frac{1}{2} \rho U^2 A = 0.0014 \times \frac{1}{2} \times 1020 \times 6.688^2 \times 43200$$
$$= 1.449 \times 10^6 \text{ N}$$

OR, 1.449 MN

$$(b) \quad P = F_D \cdot U = 1.449 \times 10^6 \times 6.688$$
$$= 9.689 \times 10^6 \text{ (W)}$$

OR, 9.689 MW

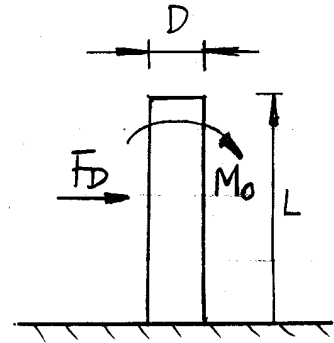
Example on Aerodynamic Drag on a Chimney (Example 9.6)

Given: $D = 1 \text{ m}$, $L = 25 \text{ m}$

$V = 50 \text{ km/hr}$, $P = 101 \text{ kPa}$

$T = 15^\circ \text{C}$

Find: Bending moment M_0 at the base



Solution:

Assume that the drag force is uniformly distributed along the chimney height. Therefore, the bending moment M_0 acting at the base of the chimney can be calculated using the total resultant drag force at the midpoint.

$$M_0 = F_D \cdot \frac{L}{2}$$

considering that $C_D = \frac{F_D}{\frac{1}{2} \rho V^2 A}$

$$\Rightarrow M_0 = C_D \cdot \frac{1}{2} \rho V^2 A \cdot \frac{L}{2} = C_D A \cdot \frac{L}{4} \rho V^2$$

$$V = 50 \frac{\text{km}}{\text{hr}} = 50 \times \frac{1000}{3600} = 13.9 \frac{\text{m}}{\text{s}}$$

with the standard air condition,

$$\rho = 1.23 \frac{\text{kg}}{\text{m}^3}, \quad \mu = 1.79 \times 10^{-5} \text{ Pa}\cdot\text{s}$$

$$Re = \frac{\rho V D}{\mu} = \frac{1.23 \times 13.9 \times 1}{1.79 \times 10^{-5}} = 9.55 \times 10^5$$

From Figure 9.13,

$$C_D = 0.35$$

The frontal area of the cylinder

is: $A = DL = 1 \times 25 = 25 \text{ (m}^2\text{)}$

$$\therefore M_0 = C_D A \frac{L}{4} \rho V^2$$

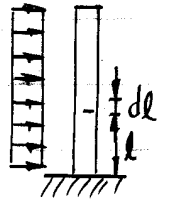
$$= 0.35 \times 25 \times \frac{25}{4} \times 1.23 \times 13.9^2$$

$$= 12996.4 \text{ (N}\cdot\text{m)}$$

OR, $12.966 \text{ kN}\cdot\text{m}$

Proof of $M_0 = F_D \cdot \frac{L}{2}$

Drag force is uniformly distributed along L ,



Moment produced by local drag force at l is:

$$m_0 = (f_D \cdot dl) \cdot l = f_D l \cdot dl$$

Total moment:

$$M_0 = \int_0^L m_0 dl = \int_0^L f_D \cdot l \cdot dl$$

$$= f_D \cdot \frac{L^2}{2}$$

B/C $F_D = \int_0^L f_D dl = f_D \cdot L$

$$\therefore M_0 = f_D \cdot \frac{L^2}{2} = F_D \cdot \frac{L}{2}$$

Example of Aerodynamic Drag on an Automobile Drag Parachute (Example 9.7)

Given: $V_0 = 270 \text{ mph}$

$V_f = 100 \text{ mph}$

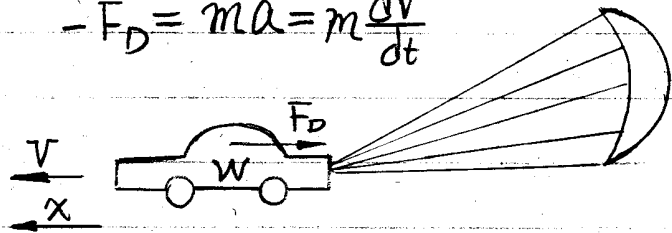
Car weight:

$W = 1600 \text{ lbf}$

Area of drag chute: $A = 25 \text{ ft}^2$

$\rho = 0.00238 \text{ slug/ft}^3$

$-F_D = ma = m \frac{dV}{dt}$



Find: time t required to slow down

Solution: By convention, we keep F_D positive. Therefore according to Newton's second law:

$$\left. \begin{aligned} -F_D = ma = m \frac{dV}{dt} \\ C_D = \frac{F_D}{\frac{1}{2} \rho V^2 A} \end{aligned} \right\} \Rightarrow -\frac{1}{2} C_D \rho V^2 A = m \frac{dV}{dt}$$

Integrating, we obtain:

$$-\frac{1}{2m} C_D \rho A \int_0^t dt = \int_{V_0}^{V_f} \frac{1}{V^2} dV$$

$$-\frac{1}{2m} C_D \rho A t = -\frac{1}{V} \Big|_{V_0}^{V_f} = -\frac{1}{V_f} + \frac{1}{V_0} = -\frac{V_0 - V_f}{V_f V_0}$$

$$\therefore t = \frac{V_0 - V_f}{V_f V_0} \frac{2m}{C_D \rho A} \left. \begin{aligned} m = \frac{W}{g} \end{aligned} \right\} \Rightarrow t = \frac{V_0 - V_f}{V_f V_0} \frac{2W}{C_D \rho A g} \quad \text{--- (1)}$$

Model the drag chute as a hemisphere, with a frontal area of $A = 25 \text{ ft}^2$.

Estimate the Reynolds number

Diameter of the frontal area: $\frac{\pi D^2}{4} = 25$

$\therefore D = 5.64 \text{ (ft)}$

Average speed $\bar{V} = (V_f + V_0)/2 = (270 + 100)/2 = 185 \text{ mph}$

1 mile = 5280 ft

$$\text{Therefore, } \bar{V} = 185 \times 5280 \times \frac{1}{3600} = 271.33 \text{ (ft/s)}$$

$$\text{From Table A.9, } \nu = 1.57 \times 10^{-4} \text{ ft}^2/\text{s}$$

$$\text{Average Reynolds number, } \bar{Re} = \frac{\bar{V} \cdot D}{\nu} = \frac{271.33 \times 5.64}{1.57 \times 10^{-4}} = 9.75 \times 10^6$$

$\bar{Re} > 10^3$, therefore, we can use Table 9.3 to determine C_D value, which is: $C_D = 1.42$

$$\text{Local gravitational acceleration: } g = 32.2 \text{ ft/s}^2$$

$$V_f = 100 \text{ mph} = 100 \times 5280 / 3600 = 146.67 \text{ (ft/s)}$$

$$V_0 = 270 \text{ mph} = 270 \times 5280 / 3600 = 396 \text{ (ft/s)}$$

From Eqn. (1),

$$t = \frac{V_0 - V_f}{V_f V_0} \cdot \frac{2W}{C_D \rho A g} = \frac{396 - 146.67}{396 \times 146.67} \cdot \frac{2 \times 1600}{1.42 \times 0.00238 \times 25 \times 32.2} = 5.05 \text{ (s)}$$

Note that we use the averaged Reynolds number. Strictly speaking, in order to use table 9.3, even at the lowest speed $V_f = 100 \text{ mph}$, Re should be larger than 10^3 .

Check:

at $V_f = 100 \text{ mph}$,

$$Re_f = \frac{V_f \cdot D}{\nu} = \frac{146.67 \times 5.64}{1.57 \times 10^{-4}} = 5.27 \times 10^6$$

which is still much larger than 10^3 .